Basin Research

Basin Research (2010) 22, 918–932, doi: 10.1111/j.1365-2117.2009.00446.x

Magnetochronology of synorogenic Miocene foreland sediments in the Fars arc of the Zagros Folded Belt (SW Iran)

Sh. Khadivi,*† F. Mouthereau,*‡ J.-C. Larrasoaña,§,[1] J. Vergés,§,[1] O. Lacombe,* E. Khademi,¶ E. Beamud, ‖ M. Melinte-Dobrinescu** and J.-P. Suc††

*Institut des Sciences de la Terre et de l'Environnement de Paris, Université Pierre et Marie Curie, Paris Cedex 05, France

†National Geoscience Database of Iran, Tehran, Iran

‡Centre de Recherches Pétrographiques et Géochimiques, Vandœuvre-lès-Nancy, France

§Institute of Earth Sciences Jaume Almera, CSIC, Barcelona, Spain

¶Geological Survey of Iran, Shiraz, Iran

‖Paleomagnetic Laboratory, Institute of Earth Sciences Jaume Almera, UB-CSIC, Barcelona, Spain

**National Institute of Marine Geology and Geo-ecology (GEOECOMAR), Bucharest, Romania

††Laboratoire PaléoEnvironnements & PaléobioSphère, Université Lyon 1, Campus de La Doua, Villeurbanne Cedex, France

ABSTRACT

The timing of deformation in the northern Zagros Folded Belt is poorly constrained because of the lack of an accurate absolute chronology of the syntectonic sedimentary sequences. The foreland basin infill in the northern part of the Fars arc is composed of supratidal sabkha deposits (Razak Fm), medium-grained deltaic deposits (Agha Jari Fm) and coarse conglomerates of nearshore fan delta deposits at the base (Bakhtyari Fm, Bk1) and continental alluvial deposits at the top of the section (Bakhtyari Fm, Bk2). A magnetostratigraphic study was carried out in a composite section spanning about 1300 m on the northern flank of the Chahar–Makan syncline. Magnetostratigraphic correlation of the Razak Fm with chron C6n yields an age of 19.7 Ma at the base of the composite section. The transition to Agha Jari Fm is correlated with chron C5Cn, yielding an age of 16.6 Ma. The transition to the conglomerates of the Bakhtyari Fm (Bk1) correlates with the chron C5AD at approximately 14.8 Ma, which is considerably older than previously thought. The base of the Bakhtyari Fm growth strata, and thus the beginning of the deformation in northern Fars, is dated at 14–15 Ma. The topmost preserved Bakhtyari Fm (Bk1) is folded and unconformably overlain by Bakhtyari Fm (Bk2) conglomerates. This indicates that tectonic deformation in northern Zagros was already underway in the Middle Miocene.

INTRODUCTION

Chronostratigraphic constraints within foreland sequences are critical for understanding the growth of orogenic systems. They are commonly used to assess the timing and rates of shortening and deposition. Along with provenance studies in the foreland and thermochronological constraints in the hinterland, the stratigraphic ages account for the evolution of tectonic accretion and sediment fluxes, and thus help to distinguish between tectonic and climatic forcing on the foreland stratigraphy.

Correspondence: Sh. Khadivi, Institut des Sciences de la Terre et de l'Environnement de Paris, Université Pierre et Marie Curie, T. 45-46, E2, Box 129, 75252 Paris Cedex 05, France. E-mail: shokofeh.khadivi@upmc.fr

[1] Present address: Instituto Geológico y Minero de España, c/ Manuel Lasala 44, 9B, 50006 Zaragoza, Spain.

Magnetostratigraphy is an appropriate technique for dating nonmarine deposits, which is particularly important when other methods are not feasible. Successful examples of dating foreland basin deposits through magnetostratigraphy include fold-thrust belts such as the Himalaya (Burbank & Reynolds, 1988), Andes (Jordan & Alonso, 1987; Reynolds *et al.*, 1990), Alps (Schlunegger *et al.*, 1997), Pyrenees (Burbank *et al.*, 1992), Tien Shan (Heermance *et al.*, 2007) and Zagros (Homke *et al.*, 2004; Emami, 2008).

The Zagros Folded Belt (ZFB), in southwest Iran, results from the closure of the Neo-Tethys ocean between the Arabia margin and the Eurasia continent (Stocklin, 1968; Koop & Stoneley, 1982). The collision belt extends over 2000 km in a NW–SE direction from eastern Turkey to the strait of Hormoz in southern Iran (Fig. 1a). Based on the reconstruction of plate circuits, McQuarrie *et al.*

(2003) suggested that plate convergence rates of 2–3 cm yr^{-1} between Arabia and Eurasia have held since ~56 Ma. According to the same authors, true continental collision started no later than 10 Ma. The present-day convergence is oriented N–S at a rate of 2.2–1.5 mm yr^{-1} and decreasing westwards, as suggested by recent geodetic surveys (Vernant *et al.*, 2004).

Our understanding of Zagros foreland continental sequences has suffered considerably from the lack of accurate stratigraphic dating. Based on biostratigraphic dating available in the Fars region (James & Wynd, 1965), the onset of deposition of siliciclastic sediments in the foreland succession is thought to have started roughly 28 Ma ago (Chattian–Late Oligocene) in the proximal Zagros foreland basin, and between 20 and 16 Ma (Burdigalian–Langhian–Early Miocene) in its distal part, consistent with the migration of foreland sequences forelandwards (e.g., Mouthereau *et al.*, 2007). The increasing flux of siliciclastic deposits represented by the Razak Formation, Mishan Formation and Agha Jari Formation of the Fars group points to the start of the overfilled stage in the Zagros foreland basin. The Miocene foreland basin development is confirmed by the noticeable increase in the thickness of the Fars group sediments northwards (Motiei, 1993; Mouthereau *et al.*, 2007). The lack of chronostratigraphic constraints in the upper continental successions has been partially solved, thanks to recent magnetostratigraphic studies carried out in the distal part of the foreland. In the Lorestan area, magnetostratigraphy has dated the initiation of folding at about 7.6 Ma ago (Homke *et al.*, 2004). A similar study suggests older ages of 11 Ma for initiation of folding in the inner part of the Zagros belt (Emami, 2008) (see Fig. 1a). The conglomerates of the Bakhtyari Formation unconformably overlie the older foreland strata. However, the age of these conglomerates is still a matter of debate. Biostratigraphic control on underlying successions led James & Wynd (1965) to propose a Late Pliocene or younger age. In the distal part of the Zagros foreland, ages of 3 Ma have also been proposed for the base of the Bakhtyari conglomerates (Homke *et al.*, 2004). In the southern Fars, a recent study argued for a minimum depositional age of 0.8–0.5 Ma based on cosmogenic dating, combined with local palaeomagnetic constraints on Bakhtyari conglomerates (Oveisi *et al.*, 2009). However, such alluvial deposits are expected to be largely diachronous throughout the foreland. It is thus not surprising that recent micropalaeontological dating and pollen stratigraphy within marine beds of the Bakhtyari Formation found in the High Zagros point to an Early Miocene and even Late Oligocene age (Fakhari *et al.*, 2008).

Despite these earlier works, two major questions remain to be solved. The ages of synorogenic foreland deposits are still not reliably constrained in the northern proximal portions of the Zagros foreland. The recent stratigraphic constraints on the Bakhtyari Formation in the High Zagros are far from the Fars area and may be related to the development of a basin restricted to the northern Zagros. The purpose of this study is to introduce new chronostratigraphic constraints on synorogenic deposits of the proximal Zagros foreland. These results are then used to assess the timing of folding in the northern ZFB.

GEOLOGICAL SETTING

Main structural features of the ZFB

The collision suture zone is marked along the Main Zagros Thrust (MZT) by ophiolitic rocks associated with deep-water radiolarites and eruptive rocks interpreted as remnants of the obducted Neo-Tethyan ocean or associated back-arc or fore-arc crust (Stoneley, 1990; Ziegler, 2001) (Fig. 1a). The metamorphic Sanandaj–Sirjan belt, north of the MZT, represents the former active margin of the Iranian microplate (e.g. Agard *et al.*, 2005) (Fig. 1a). To the south, the High Zagros and the ZFB are made up of folded and thrusted Palaeozoic, Mesozoic and Tertiary sediments. The orogenic wedge *sensu-stricto* is represented by the ZFB, which is being built above two major décollement levels localized in the Cambrian salt and in the ductile mid-lower crust (Colman-Sadd, 1978; Berberian, 1995; McQuarrie, 2004; Molinaro *et al.*, 2004, 2005; Sherkati & Letouzey, 2004; Mouthereau *et al.*, 2006, 2007). In contrast, the High Zagros and the Sanandaj–Sirjan domain form a highly elevated low-relief domain on the southern edge of the Iranian plateau.

The tectonic and magmatic history of the Zagros collision can be summarized as follows: following the obduction in the upper Cretaceous and arc magmatism in the Sanandaj–Sirjan belt during the Mesozoic, the Eurasian side of the collision underwent arc magmatism in the Urumieh–Doktar belt in the Eocene (Berberian & Berberian, 1981). The timing of this last magmatic arc event is confirmed by U/Pb ages of zircon grains from magmatic plutons (Horton *et al.*, 2008) and by Eocene cooling ages reported in the Zagros foreland basin from the fission-track analysis on detrital apatites (Homke *et al.*, in press). This Eocene volcanic event is likely related to northward subduction of the Tethys, although its tectonic setting can be attributed either to Andean-type volcanism (Berberian *et al.*, 1982) or to back-arc spreading (Vincent *et al.*, 2005). On the Arabian margin, a period of subsidence is recorded by the remarkable deposition of turbidites onto previously emplaced ophiolitic units (Berberian & King, 1981; Stoneley, 1981; Hempton, 1987; Beydoun *et al.*, 1992). The two main possible causes for the subsidence observed could be either loading by the thickened northern Eurasian margin, including the fore-arc domain, or the deep-seated loading originating from the Arabian slab pull.

Despite numerous regional evidences from Irak, the Caucasus and the South Caspian basin indicating that the Arabia–Eurasia collision could have started in the Late Eocene (Vincent *et al.*, 2005; Allen & Armstrong, 2008), it seems that the beginning of contraction within the southern Zagros of our studied area did not occur before the Late Oligocene–Early Miocene. This timing is based on

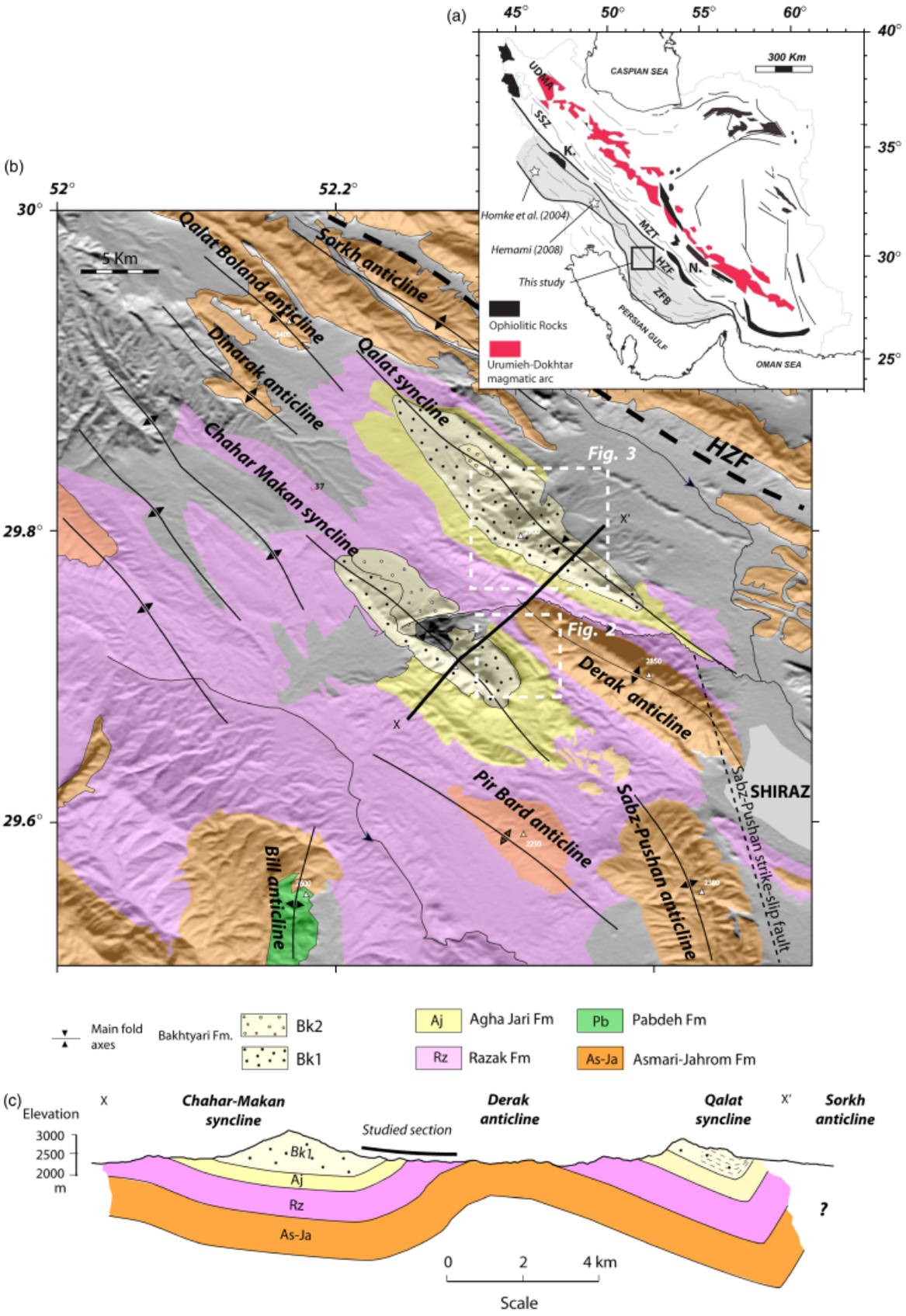

the following arguments: (1) the initiation of inversion of the Arabian margin in the Zagros basin occurred at this time (Mouthereau *et al.*, 2006, 2007; Ahmadhadi *et al.*, 2007); (2) the Iranian plateau and the Zagros basin were below sea level during the Oligocene, except for the morphological ridge formed by the stacked ophiolitic units; (3) the persistence of early Miocene flyschs in the High Zagros (Stoneley, 1981); and (4) Miocene marine incursions in the High Zagros found in close relation to the first deposition of alluvial-fan conglomerates of the Bakhtyari Formation as attested by new stratigraphic constraints (Fakhari *et al.*, 2008).

Tectonic constraints on the development of the Zagros foreland basin in the Fars Arc

Few studies have specifically focused on the history of the Zagros foreland basin in the Fars province, in part because of a missing robust chronostratigraphy, which is the purpose of this paper. In the following, we summarize the main features of its stratigraphic evolution.

Coeval with the deposition of Eocene turbidites on Arabian and Eurasian margins (Berberian & King, 1981; Stoneley, 1981; Hempton, 1987; Beydoun *et al.*, 1992; Vincent *et al.*, 2005), dolostones of the Jahrom Formation were deposited in the Zagros basin. This formation overlies a former regressive succession that ended up with subaerial deposition of the Sachun Formation (Motiei, 1993), whose age can be indirectly constrained laterally by the Kashkan Formation dated as Ypresian (~56 Ma; Homke *et al.*, 2009). The Jahrom Formation (Fig. 1b) has been deposited during an early phase of the development of the Zagros foreland basin. Although the origin of the flexure can be debated, as presented in the previous section, it occurred before the propagation of contraction into the Arabian margin (Mouthereau *et al.*, 2007).

Available stratigraphic correlations and well data (James & Wynd, 1965) also support the presence of a Middle Eocene–Late Oligocene or a Late Eocene–Lower Miocene unconformity between the Jahrom Formation and the Asmari Formation in the Fars. Because this episode preceded the overfilled stage in the Zagros basin and is related to a major transgression, the above-mentioned unconformity can be tentatively interpreted as a flexural unconformity. If this is confirmed by further stratigraphic and sedimentological studies, this unconformity could signal the initiation of the foreland basin and the beginning of the current Zagros collision. From this time onwards, more efficient plate coupling led to the thickening of the Arabian margin and its uplift (Mouthereau *et al.*, 2007). The increase of erosion on the orogenic side, together with the migration of the flexural wave into the Arabian margin, led to the deposition of a characteristic prograding foreland sequence formed by the Fars Group. This sequence is composed, in the Fars, by a synorogenic succession including the Razak Formation that conformably overlies the Asmari Formation. The Razak Formation grades upwards into the Agha Jari Formation and Bakhtyari Formation. The increase in sediment accumulation, together with the establishment of current plate velocities, likely occurred coeval with the deposition of the shallow-marine siliciclastic deposits of the Agha Jari Formation (e.g. Mouthereau *et al.*, 2007).

THE STUDIED AREA

Main structural features

The study area is located in the Fars province of Iran, in the northern part of the ZFB, 20 km to the NW of Shiraz. It is characterized by the occurrence of a trend of folds just westwards of the active Sabz–Pushan strike–slip fault (Fig. 1b). We have examined the strata within the Qalat and Chahar–Makan synclines, which are on the north and south sides of the Derak anticline (also named Qalat anticline), respectively (Mouthereau *et al.*, 2007). The Derak anticline is one of the main structural features in the area (Fig. 1b). It is oriented NW–SE, with an axial length of 20 km and a width of 10 km. The geomorphic expression of the Derak anticline is controlled by the resistant unit corresponding to the Eocene Jahrom and Late Oligocene–Miocene Asmari limestones. These series are overlain by the erodible units of the Fars Group that are well exposed in both synclines. On top of the Fars Group, the thick succession of Bakhtyari conglomerates forms topographic highs due to the large proportion of limestone pebbles that are more resistant to erosion occurring in these series. Based on field observations and analysis of SPOT 5 × 5 m resolution images, and in agreement with an earlier work (Fakhari *et al.*, 2008), two types of Bakhtyari conglomerates can be distinguished on the basis of their different structural–stratigraphic relationships. The lowest unit, called Bakthyari 1 (Bk1), is prefolding in the northern flank of the Chahar–Makan syncline (Fig. 2) but is clearly syn-folding on the northern flank of the Qalat syncline (Fig. 3). In contrast, the upper flat succession of conglomerates, named Bakthyari 2 (Bk2), appears to be mainly postfolding as it unconformably overlies the Bk1

Fig. 1. (a) Location of the studied area, with the main structural divisions, in the framework of the Arabia–Eurasia plate convergence. UDMA, Urumieh–Doktar Magmatic Arc; SSZ, Sanandaj–Sirjan Zone; MZT, Main Zagros Thrust; HZF, High Zagros Thrust; ZFB, Zagros Folded Belt. Black-filled areas correspond to ophiolites. K, Kermanshah ophiolitic group; N, Neyriz ophiolitic group. (b) Geological map of the studied area, with major structural and geological units, superimposed on the shaded topography (SRTM data). (c) Geological section across the main structural features studied e.g. Chahar–Makan, Qalat synclines and Derak anticline. Surface constraints are based on bedding dip measurements at sample sites and formation thickness (see Fig. 2 for the location of sample sites), with additional mapping based on SPOT (5 × 5 m resolution) images and DEM.

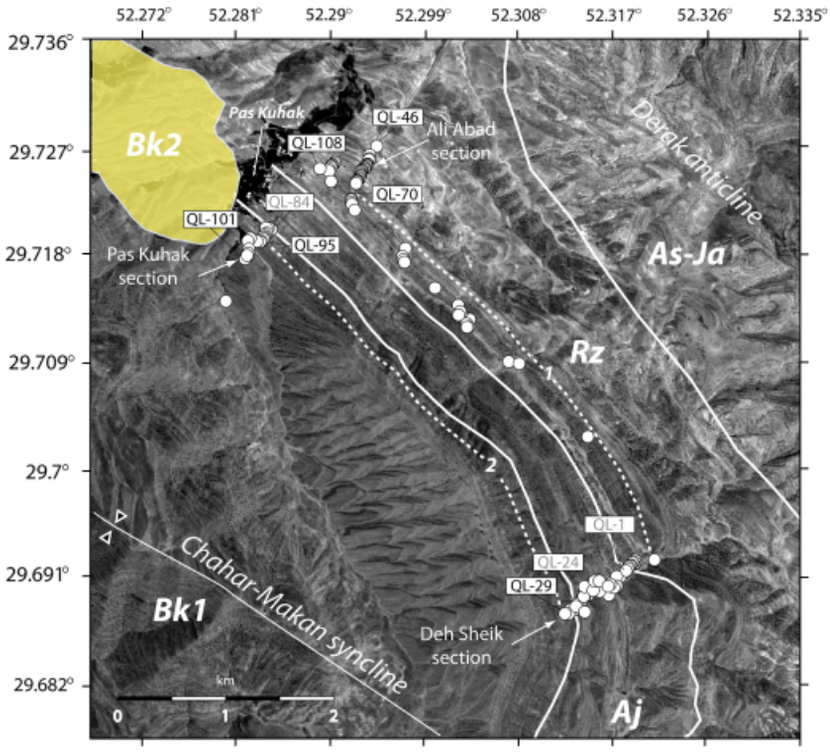

Fig. 2. (a) SPOT (5 × 5 m resolution) image of the northern flank of the Charar–Makan syncline showing the location of sections and sample sites. Boundaries between As–Ja, Asmari–Jahrom, Rz, Razak Formation, Aj, Agha Jari Formation and the Bk1, Bakhtyari Formation, as well as the correlation between each section (thick, dashed, white lines labelled 1 and 2) are also shown.

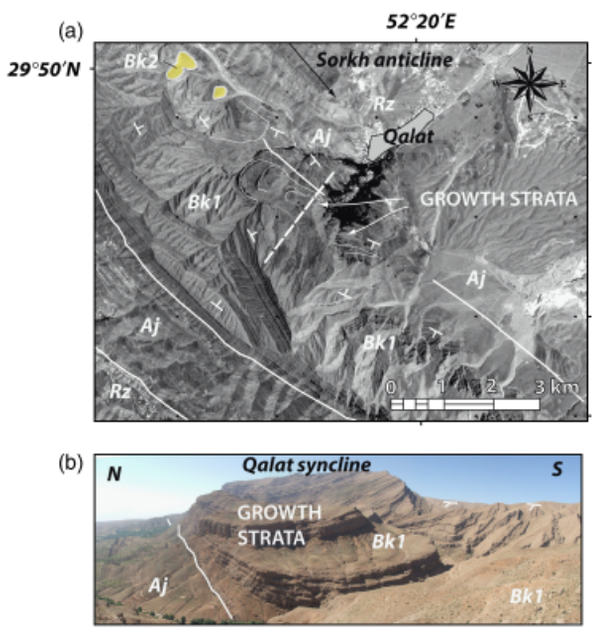

Fig. 3. (a) SPOT (5 × 5 m resolution) images and (b) field photograph of the northern side of the Qalat syncline showing the growth strata located near the base of the Bk1 conglomerates. Abbreviations are Rz, Razak Fm, Aj, Agha Jari, and Bk1 and Bk2 conglomerates correspond to both types of Bakhtyari conglomerates distinguished on the basis on their different structural positions and sediment facies.

conglomerates in the core of both the Qalat and the Chahar–Makan synclines (Figs 2 and 3).

In spite of local evidence for salt-related deformation within the Razak Formation to the SE of the studied area, both the Razak and the Agha Jari Formations conformably overlie the Asmari limestones. No major fault has been recognized from field observations or based on SPOT images. The most remarkable active feature is found to the East and corresponds to the 160°N right-lateral Sabz–Pushan fault, which is the most likely source of considerable damage and deaths in the city of Shiraz and Qalat village related to a major historical earthquake (Ms = 6.4) in 1824 (Ambraseys & Melville, 1982; Berberian, 1995).

Regular measurements of structural dips in the field and the calculation of dips based on SPOT images indicate that the northern flank of the Chahar–Makan syncline is dipping roughly 50°S, whereas its southern flank gently dips 30°N (Fig. 1b). Such an asymmetry also characterizes the Qalat syncline, the bedding on the northern flank being steeper than that on the southern one. The extraordinary preservation of synorogenic deposits, together with evidence of local syn-folding unconformities (Bk1) and postfolding unconformities (Bk2), makes this area the perfect target to carry out magnetostratigraphy in the northern Fars.

The studied sections

On the northern flank of the Chahar–Makan syncline, three main sections have been studied in order to obtain a complete succession from the Razak Formation to the lowermost part of the Bakhtyari Bk1 conglomerates (Fig. 4). The first section, named the Ali Abad section, includes ~500 m of Razak Formation made up of blue and red clays interbedded with yellow calcareous sandstone sheets (10 cm–2 m thick) with occasional gypsum beds on top (< 1 m thick) (Fig. 5a). These sediments are interpreted to be deposited in coastal lagoons and supratidal sabkha

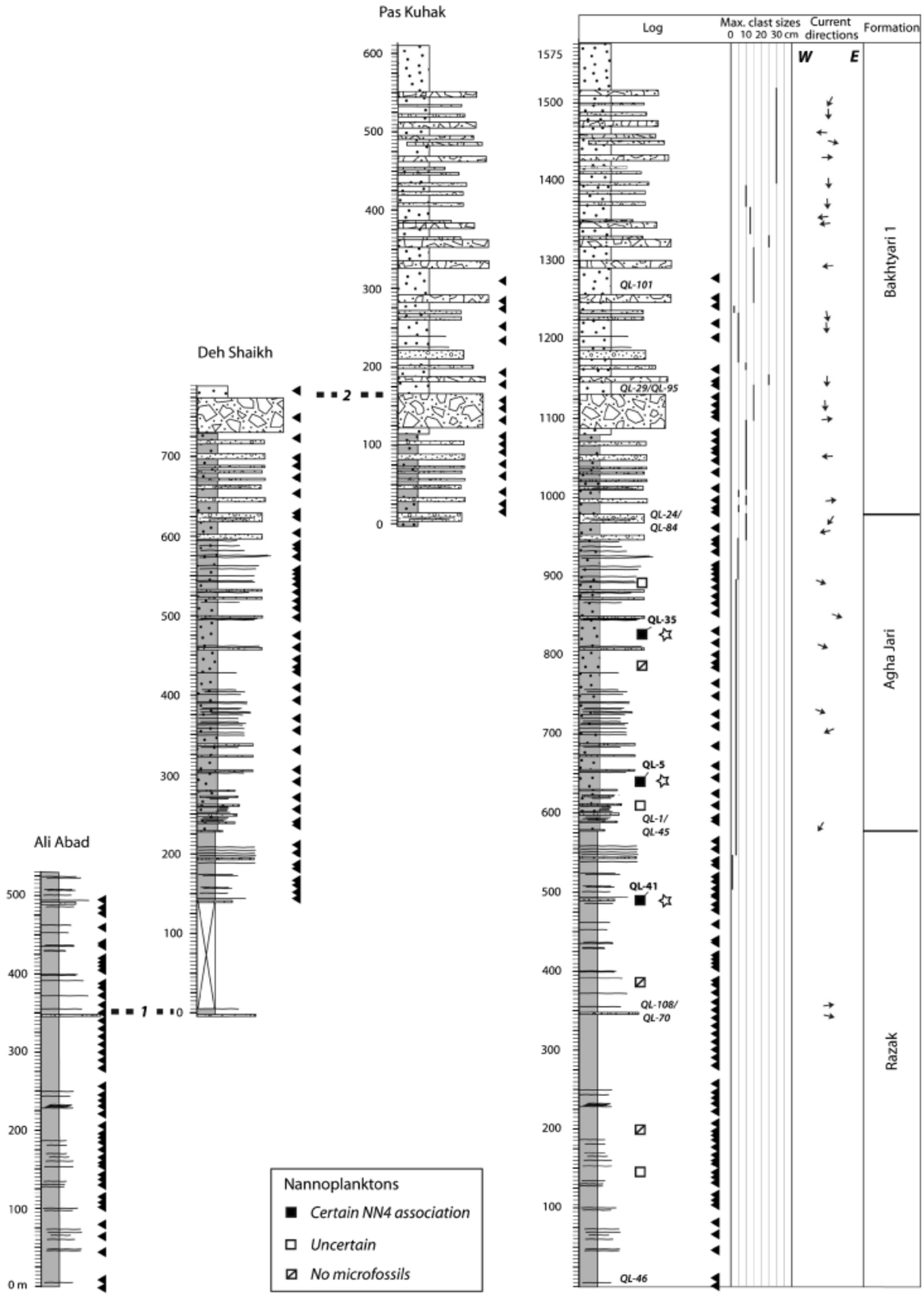

Fig. 4. Correlation between the studied stratigraphic subsections Pas Kuhak, Ali Abad and Deh Sheik, used to construct the composite magnetostratigraphic Chahar–Makan section shown in Fig. 7. Positions of samples located in Fig. 2 are indicated by black triangles. On the right of the composite stratigraphic section, we present the evolution of measured grain sizes and current orientations. The nine nannoplankton samples studied are also presented according to whether they have yielded a certain determination of the NN4 biozone such as QL-5, QL-35 and QL-41 (black-filled boxes; see also Fig. 9), uncertain determination (white-filled boxes) or no microfossils (cross white-filled boxes). The position of samples bearing dinokysts is also shown (open stars). Horizontal, black, dashed lines represent key beds (1, 2) that have been used for correlation between studied subsections (see locations in Fig. 2).

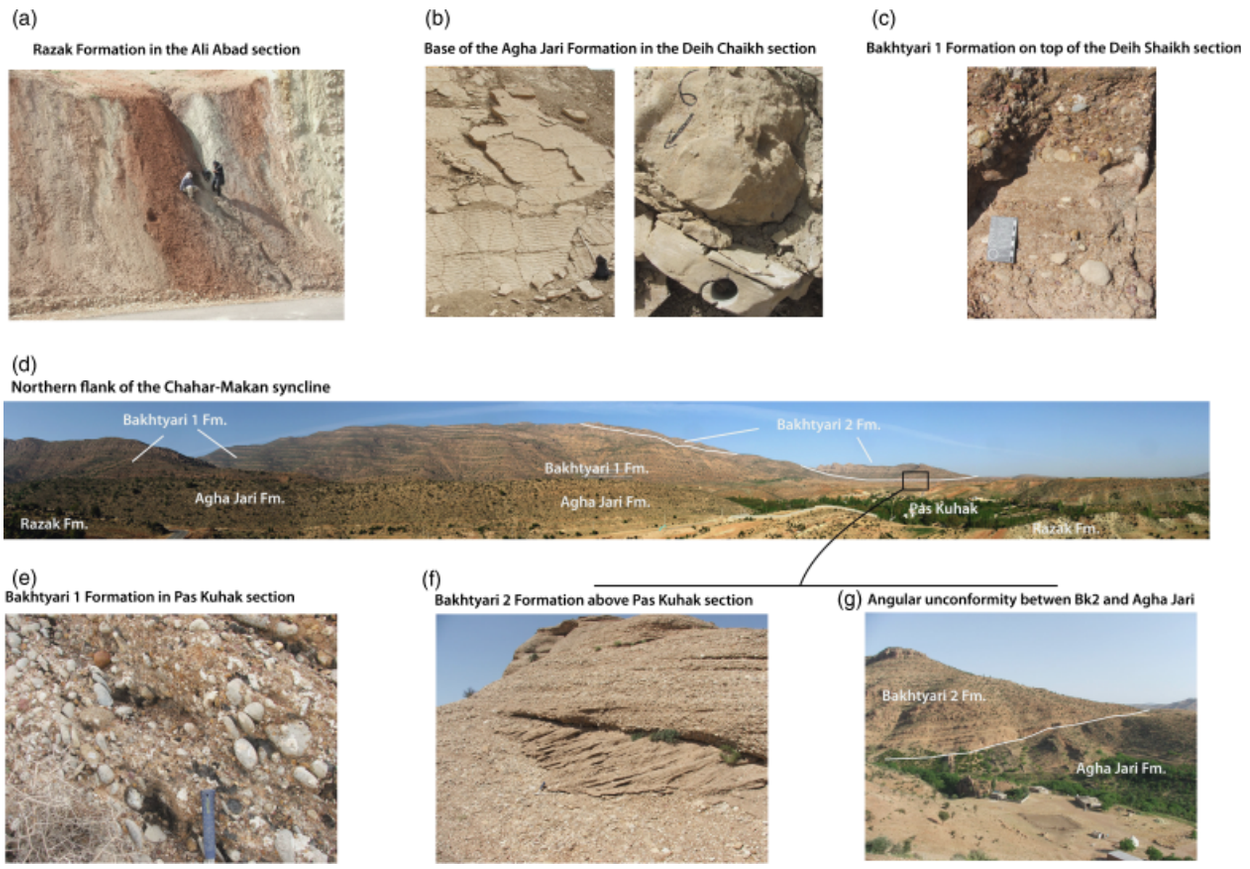

Fig. 5. Photographs of key outcrops in the sampled formations. (a) Alternating blue-to-yellow mudstones with thin beds of limestones, thin sandstones and dolostones typical of the Razak Formation (Ali Abad section). (b) Base of the Agha Jari Formation in the Deh Shaikh section. Sedimentary structures such as current ripples confirm the marine origin of the basal Agha Jari Formation. (c) Conglomerates of the Bakhtyari 1 Formation in the Deh Shaik section. The red colour of the matrix indicates the abundance of radiolarian cherts rather than weathering. The facies correspond to clast-supported, poorly to very poorly sorted gravels to cobbles interbedded with coarse sandstones showing through crossstratification. They were deposited in a coastal fan delta. (d) Panorama of the studied area striking N–S (right side) to E–W (in the centre of the image). (e) Clast-supported stratified cobbles and gravels in the Bakhtyari 1 with clast imbrications in the Pas Kuhak section. (f) Bakhtyari 2 conglomerates. The facies consists of clast-supported poorly to well-sorted planar alignments of 5–10 cm well-rounded massive gravels associated with gravels with planar through cross bedding. They can be interpreted as a subaqueous sheet flood in alluvial fan related to migrating bar forms. (g) The angular unconformity between Bakhtyari 2 conglomerates and the Agha Jari formation, west of the Pas Kuhak village. The unconformable contact between Bk1 and Bk2 can be inferred from the panorama view in (d) and is consistent with the satellite image presented in Fig. 2.

environments; their cyclic evolution is related to the episodic connection with open marine environments.

The second section, named the Deh Shaikh section, was sampled in the same structural domain but 4 km to the SE, where the transition between the uppermost part of the Razak Formation and the Agha Jari Formation was accessible. The Deh Shaikh section includes about 100 m of Razak Formation, which grades progressively upwards into the Agha Jari Formation. The outcropping ~400 m of the Agha Jari Formation is composed of reddish sandstones and metre-scale conglomeratic sheets interbedded with thick (up to 20 m) intervals of red siltstones. Sandstone beds are often thicker than 2–3 m, and conglomerates include limestone cobbles of Palaeogene and Cretaceous formations of up to 10 cm (Fig. 4). The presence of bidirectional current ripples and frequent cross-bedding laminations in sandstones (Fig. 5b) in the lower part suggests a deltaic environment; an open marine connection is confirmed by the presence of nannoplankton (Fig. 4). Measurements of current directions suggest local longitudinal currents parallel to the axis of the foreland basin. The upper part of the Deh Shaikh section includes the lowermost ~150 m of the Bakhtyari 1 conglomeratic succession (Figs 4 and 5c).

The third section, named Pas Kuhak, is located south of the Pas Kuhak locality (Figs 4 and 5d). This section includes ~600 m of sandstones and red silts with frequent conglomeratic beds that can be up to 40 m thick. The conglomerates are clast-supported, poorly sorted and well rounded (Fig. 5e). They are arranged as thick channel-like conglomeratic beds intercalated with trough cross bedding in sandstones. This type of facies association suggests the predominance of subaqueous debris flows and migrating barforms. They likely correspond to an alluvial fan deposited in a fluvial-dominated deltaic environment, whose facies appears characteristic of the Bakhtyari Formation.

In the following, we refer to this formation as Bakhtyari 1 (Bk1) in order to differentiate it from Bakhtyari 2 (Bk2), which corresponds to the upper Bakhtyari conglomerates of alluvial origin lying unconformably above Bk1 conglomerates (Fig. 5f, g). Clasts of the Bakhtyari 1 Formation are typically made up of radiolarian cherts (< 10 cm) and well-rounded pebbles of Mesozoic limestones and Nummulitic limestone of the Jahrom Formation, with diameters up to 30 cm (Fig. 4). Current markers show a more pronounced southward flow, oblique to the main structural patterns.

Stratigraphic correlations between all sections were constrained by combining field mapping, SPOT images and aerial photographs. The correlation between the Ali Abad and the Deh Shaikh sections is based on the presence of a distinctively thick package of calcareous sandstone beds that appears at metre ~350 in the Ali Abad section and is found ~150 m below the lowermost sampled site in the Deh Shaikh section. The correlation between the Deh Shaikh and the Pas Kuhak sections is based on the presence of a distinctively thick (50 m) package of conglomerates. Correlation between the three sections enables the construction of a composite section, named Chahar–Makan, with a total thickness of 1575 m.

MAGNETOSTRATIGRAPHY

Sampling strategy

A total of 46, 45 and 18 palaeomagnetic sites were sampled using a portable gas-powered drill along the Ali Abad, Deh Shaikh and Pas Kuhak sections, respectively. The total number of 109 sites is distributed along 1450 m of sedimentary succession, which corresponds to the lowermost 1275 m of the Chahar–Makan composite section and results in a mean sampling resolution of 12 m. Considering mean accumulation rates of 20–30 cm kyr^{-1} reported by Homke *et al.* (2004) for foreland sediments of the Zagros in the Lurestan region, this resolution corresponds to an estimated mean of one sample per 40–60 kyr. More than 85% of polarity intervals in the Lower and early Middle Miocene have a duration longer than 120 kyr (Lourens *et al.*, 2004). Therefore, our sampling strategy is likely to resolve most polarity intervals with at least two consecutive samples in spite of difficult logistic and outcrop conditions, which prevented tighter sampling. The presence of thick conglomerate beds and covered mudrock intervals in the upper and lower parts of the section, respectively, has determined the presence of some sampling gaps of up to 30 m. Palaeomagnetic sampling was focused on fine-grained lithologies such as blue mudstones, red siltstones and fine-grained sandstones. Because of the scarcity of such suitable lithologies in some parts of the section, carbonates and coarse-grained sandstones were also drilled in the middle part of the Razak Formation and in the Bakhtyari 1 conglomerates. Nine samples for nannoplankton dating were collected from marine sediments located around the transition between Razak and Agha Jari formations, in order to provide independent age constraints.

Palaeomagnetic analyses were performed using a 2G superconducting rock magnetometer at the Institute of Earth Sciences 'Jaume Almera' in Barcelona (Spain). The noise level of the magnetometers is $< 7 \times 10^{-6}$ A m^{-1}, which is much lower than the magnetization of the samples measured. The thermal treatment involved between eight and 16 steps at intervals of 100°, 50 °C, 30 °C and 20 °C to a maximum temperature of 690 °C. Demagnetization of a set of pilot samples representative for all the lithologies studied allowed optimization of the demagnetization steps to allow accurate calculation of the Characteristic Remanent Magnetization (ChRM) directions, minimizing heating and the formation of new magnetic phases in the oven. ChRM directions were identified through visual inspection of vector endpoint diagrams of demagnetization data (Zijderveld, 1967). Based on their demagnetization pattern, ChRM directions have been divided into three groups. Type 1 magnetizations are those that describe well-defined linear trends directed towards the origin of the demagnetization plot, which enables a very accurate calculation of their directions. Type 2 magnetizations are those that display less-developed linear trends, and yet they enable a reliable calculation of their directions. Type 3 magnetizations are those that display either poorly developed directions or incomplete demagnetizations due to the growth of new magnetic minerals in the oven, and yet they provide reliable polarity determinations by fitting clustered directions to the origin of the demagnetization plots. Magnetization directions were calculated using principal component analysis (Kirschvink, 1980).

Palaeomagnetic results

In most of the samples, a low-temperature magnetic component is unblocked below 250–300 °C (Fig. 6). This component is parallel to the present-day field in the region (Dec = 0°, Inc = 46°) in geographic coordinates, and is interpreted as a viscous component with no geological meaning. Above this temperature, a ChRM can be identified in about 65% of the studied samples. About 10, 33 and 22% of ChRM directions belong to quality types 1, 2 and 3, respectively. Unblocking temperatures range between ~500 °C and 690 °C in red siltstones, some grey mudrocks and fine-grained sandstones from the Razak, Agha Jari and Bakhtyari 1 formations (Fig. 6d, g), which points to haematite as the main magnetic carrier. In limestones and most grey mudrocks of the Razak Formation, the ChRM is unblocked below 500 °C (Fig. 5e), which points to magnetite as the main carrier. The ChRM shows northerly and southerly directions with shallow inclinations in geographic coordinates, which become similar to the Miocene reference direction for the area studied (Dec = 0.7°; Inc = 39.8°; α_{95} = 5.8°; see Smith *et al.*, 2005) after tilting the beds back to their initial horizontal position (Fig. 7). Although no significant results are obtained when per-

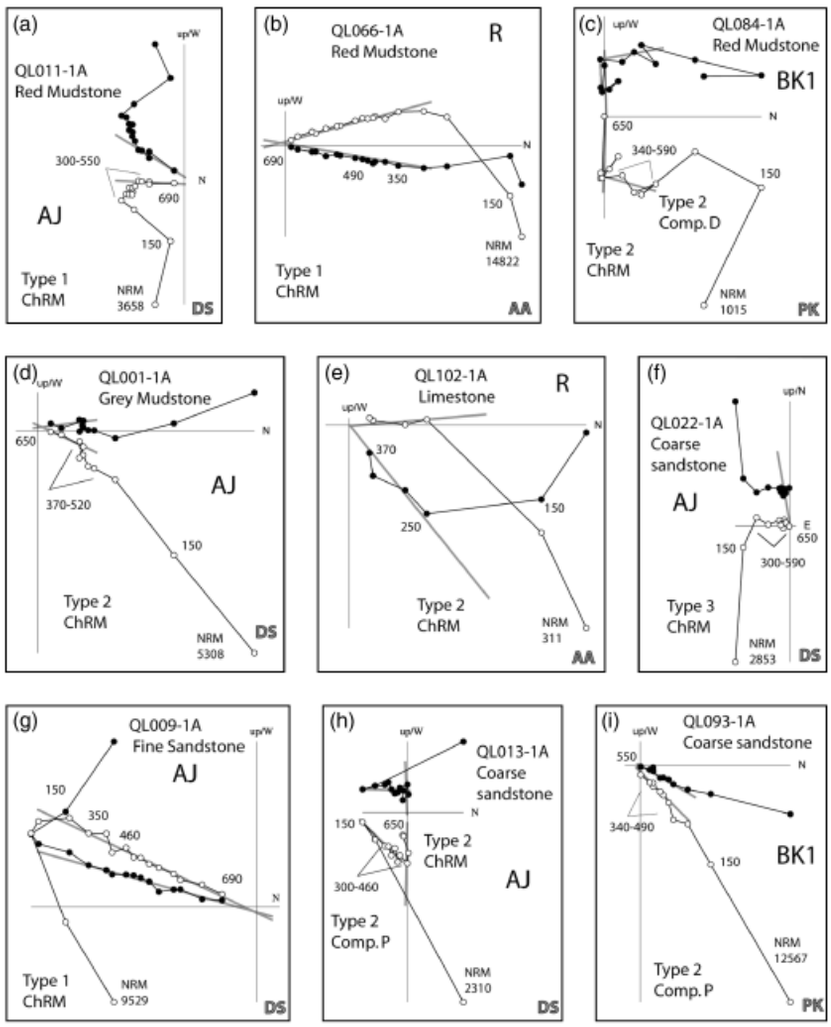

Fig. 6. Demagnetization plots representative of the different types of rocks and sedimentary formations studied. Grey lines represent the linear fit to the calculated directions. Demagnetization plots are in geographic coordinates, the temperature steps in degrees Celsius C and the intensity of the NRM in 10^{-6} A m^{-1}. The quality of the palaeomagnetic directions for the ChRM and components D and P has been indicated. AJ, Agha Jari; R, Razak; BK1, Bakhtyari 1; AA, Ali Abad; DS, Deh Shaikh; and PK, Pas Kuhak.

forming the fold test due to the similar dip of all the studied beds, this strongly suggests that the ChRM was acquired before folding. In palaeogeographic coordinates, normal and reversed ChRM directions of quality types 1 and 2 pass the reversal test with class C (McFadden & McElhinny, 1990), which reinforces the interpretation that the ChRM represents a primary magnetization acquired at, or shortly after, deposition of the studied rocks. Only in some cases does the ChRM seem to show a complex behaviour so that an additional prefolding component is unblocked below 590 °C (Fig. 6c,h). This component, named D, displays a polarity opposite to the higher temperature ChRM, and is interpreted as a delayed magnetization acquired most probably around polarity transitions. The results described here for the ChRM of the Razak, Agha Jari and Bakhtyari formations are similar to those reported in previous studies (Homke *et al.*, 2004; Smith *et al.*, 2005; Aubourg *et al.*, 2008; Emami, 2008).

In about 18% of the studied samples, typically coarse-grained sandstones of the Agha Jari and Bakhtyari 1 formations, an additional stable magnetization is found. This component, named Component P, displays normal and reverse polarity directions (Fig. 6h, k) that often obliterate the initial ChRM direction (Fig. 6k). Component P is similar to the remagnetization reported for similar rock types in the Fars by Smith *et al.* (2005) and Aubourg *et al.* (2008), who interpreted it to be of sub-recent origin on the basis of its normal polarity (Fig. 7). Our results indicate, however, that Component P displays both normal and reverse polarity directions that conform to the Miocene–Pliocene reference directions for the studied area before, but not after, tectonic correction (Fig. 8). This indicates that Component P is a postfolding remagnetization acquired before, at least, 0.78 Ma.

virtual geomagnetic pole (VGP) directions have been calculated using ChRM directions of quality types 1, 2 and 3. The obtained VGP latitudes provide a sequence of polarity changes for the Chahar–Makan composite section in which polarity intervals have been determined by at least two consecutive samples (Fig. 8). The established sequence includes eight normal magnetozones, which have been labelled N1–N8 from bottom to top, and seven reverse magnetozones, which have been labelled R1–R7 (Fig. 8). The most conspicuous patterns of this polarity sequence are a long normal polarity interval in the upper part of the section (N8) and a cluster of three short normal magnetozones (N4–N6) separated by two reverse intervals (R4, R5) in its middle part. In the lower part of the section,

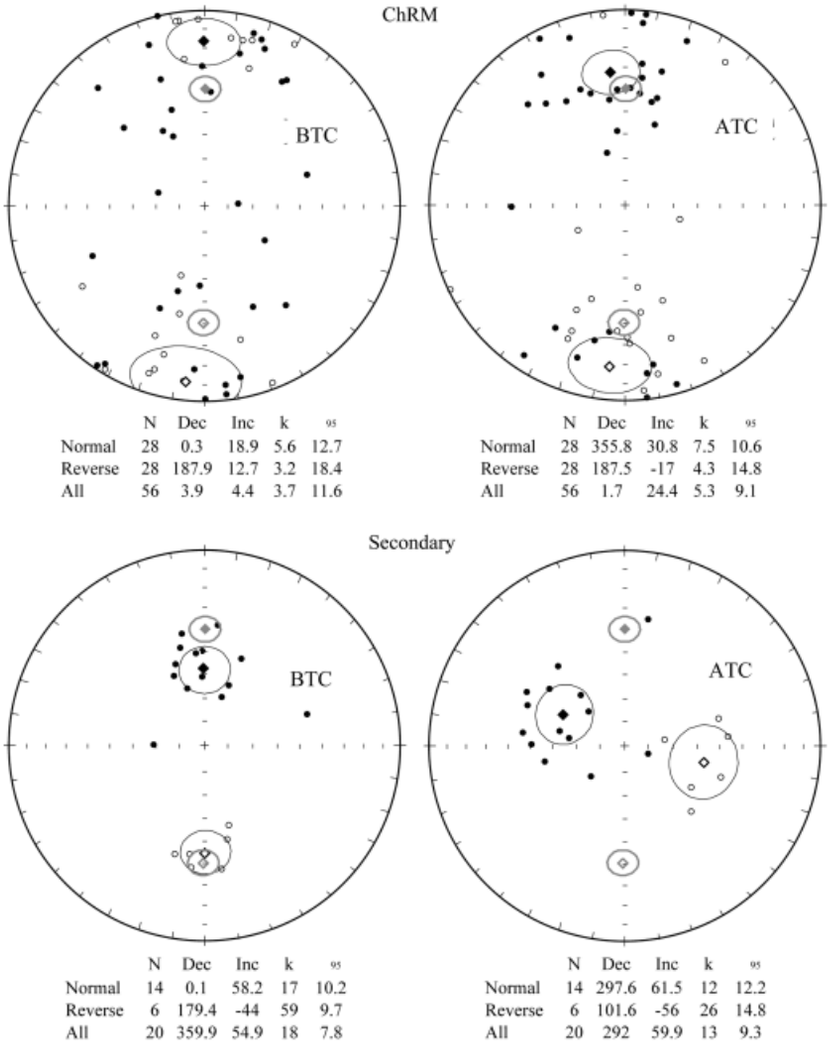

Fig. 7. Equal-area stereographic projections of the ChRM (upper panel) and component P (lower panel) directions before (BTC) and after (ATC) tectonic correction. Mean directions with the 95% confidence angle are displayed. *N*, number of directions; Dec, declination; Inc, inclination; k, precision parameter; $\alpha 95$, confidence angle. Grey symbols indicate the normal and reverse components of the Miocene reference direction in the area.

just above N2 and N1, the presence of samples with alternating normal and reverse polarities allows identification of two intervals with an uncertain polarity attribution (Fig. 8). In addition, three single-sample intervals appear just above N1 and within the upper part of R6 and N8 (Fig. 8).

Correlation with the geomagnetic polarity time scale (GPTS)

The correlation between the middle part of the Chahar–Makan composite magnetostratigraphy and the Geomagnetic Polarity Time Scale (GPTS) reported in Lourens *et al.* (2004) is straightforward based on the distinctive pattern of polarity reversals and the anchor point provided by the calcareous nannofossils. Three nannofossil samples of the Deh Shaikh section, characterized by nannoplankton assemblages with *Sphenolithus heteromorphus* (first common occurrence at about 17.7 Ma and last occurrence at about 13.6 Ma), *Cyclicargolithus foridanus* (last occurrence at 12 Ma), *Helicosphaera ampliaperta* (first occurrence at about 20.4 Ma and last occurrence at about 14.9 Ma) and *Discoaster deflandrei* (Fig. 9), can be ascribed to biozone NN4, which ranges from Burdigalian to Langhian in age (i.e. 18–14.9 Ma) (Raffi *et al.*, 2006). This constrains the characteristic triplet formed by N4–N6 to correlate with chron C5Cn, and the underlying magnetozones (R2–R3) to correlate with chrons C5Dr, C5Dn and C5Cr, respectively. Similarly, the long, overlying reverse magnetozone (R6) must correspond to chron C5Br. The correlation to the GPTS is less straightforward for the lower part of the section due to the intervals of uncertain polarity attribution. Noticeably, the two intervals with alternating normal and reverse polarity directions occur just above N1 and N2. This suggests that both N1 and N2 correspond to genuine normal polarity intervals in which reverse ChRM directions at their tops represent delayed remanences acquired after the shift in polarity was completed (Fig. 8). This behaviour, which is very common in Miocene continental deposits of the Zagros (Homke *et al.*, 2004) and other foreland basins within the Alpine–Himalayan collision belt (e.g. Larrasoaña *et al.*, 2006), is equivalent to that of Component D mentioned above, although in that case, part of the ChRM retained the original polarity. Based on our interpretation, and

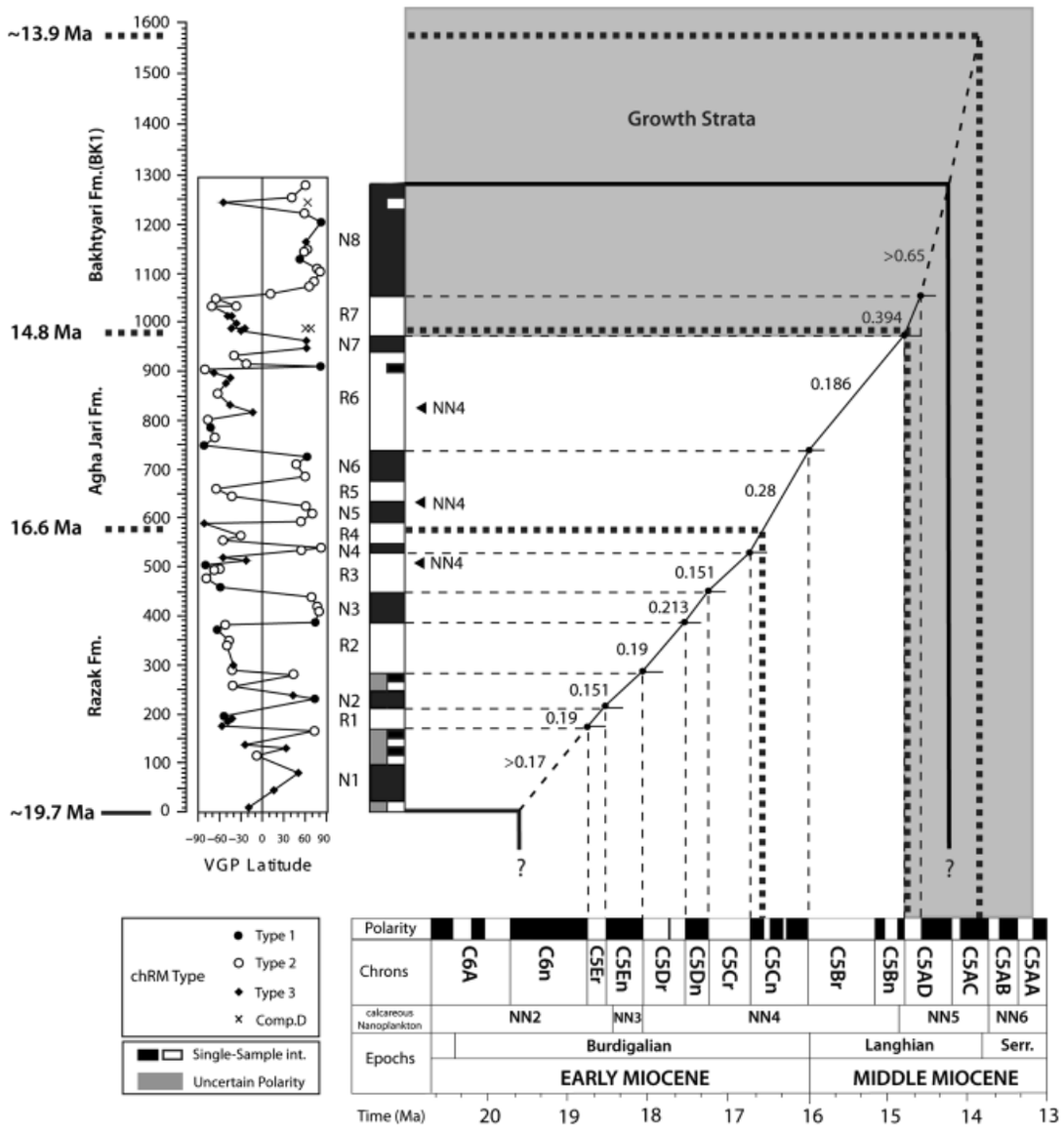

Fig. 8. Correlation of the magnetic polarity sequences of the studied Chahar–Makan section to the GPTS2004 (Lourens *et al.*, 2004). Sedimentation rates are given in mm yr^{-1}. Ages for the base of the Razak, Agha Jari and Bakhtyari 1 formations are displayed. Black triangles labelled NN4 refer to samples containing characteristic nannoplankton assemblages (see Fig. 9). The correlation of the NN4 biozone with GPTS2004 is after Raffi *et al.* (2006). The grey area shows the likely stratigraphic extent of the growth strata related to the development of the Sorkh anticline.

pinning the sequence down from R2 (chron C5Dr), intervals N1, R1 and N2 can be correlated with chrons C6n, C5Er and C5En, respectively. This solution, which is entirely consistent with the thickness pattern of the inferred magnetozones (N1–N2), implies that the base of the section is slightly younger than the C6A/C6n boundary.

Correlation of the upper part of the section to the GPTS is somewhat problematic due to the presence of single-sample polarity intervals (Fig. 8). Correlating the two normal magnetozones (N7 and N8) above R6 to the two consecutive normal chrons above C5Br (i.e. within C5Bn) results in unrealistically high sedimentation rates for the top of the section. The alternative solution, correlating N8 with C5AD.1n, implies that one of the normal events within C5Bn might be missing. Given the presence of the single-sample normal polarity interval below N7, we interpret that it might represent a poorly captured chron C5Bn.2n and that N7 correlates with C5Bn.1n. We consider this second possibility much more likely because it provides a significantly better fit with the GPTS and results in a plausible increase in the mean sedimentation rates just at the onset of Bk1 deposition. According to this interpretation, an age of 14.2 Ma (i.e. slightly older than the C5AD/C5AC boundary) can be estimated for the top of the sampled section.

The proposed solution for the Chahar–Makan composite section results in smooth accumulation rates that steadily increase from 0.17 at the base to 0.65 mm yr^{-1} at the top of the section. Our results indicate that the composite section spans from chrons C6n to C5AD (ca. 19.7–14.2 Ma),

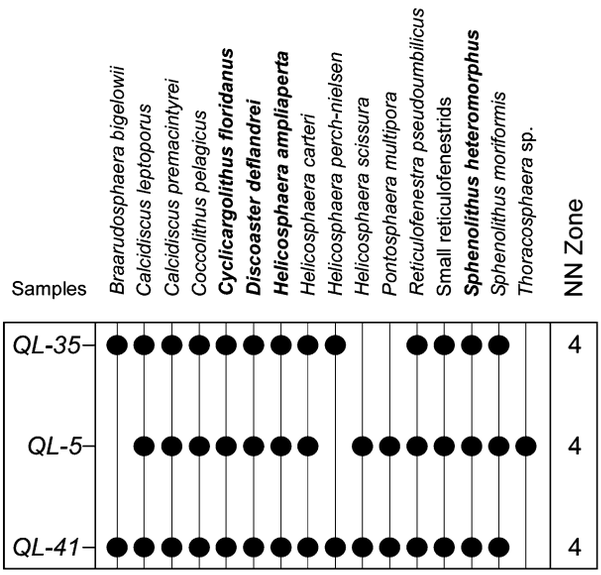

Fig. 9. Nannofossil record from three samples of the Deh Shaikh section. Biostratigraphic markers are in bold characters.

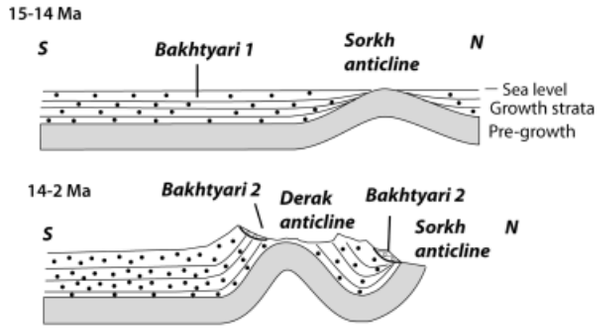

Fig. 10. Schematic reconstruction of the sequence of folding in the studied area. Magnetostratigraphic dating of the growth strata (Bakhtyari 1 conglomerates) reveals that folding in the Sorkh anticline started ca. 14–15 Ma. At this time, the Zagros Folded Belt was close to the sea level. A remarkable change occurred after 14–15 Ma and before 2 Ma (assumed base of the Bakhtyari 2 conglomerates) when the Derak anticline developed coeval with the uplift of the entire Zagros Folded Belt.

and yield an age of > 19.7, 16.6 and 14.8 Ma for the base of the Razak, Agha Jari and Bakhtyari 1 formations, respectively (Fig. 8). Based on a linear sedimentation rate upwards from the uppermost reversal, we infer an age of 13.9 Ma for the upper boundary of the logged Bakhtyari 1 conglomerates.

DISCUSSION

Age of the proximal Zagros foreland basin: implications for the development of the Zagros collision

The magnetostratigraphy carried out in this study places new constraints on the age of foreland sedimentation in the northern part of the Zagros foreland basin. The present work shows that the base of the Razak Formation is older than 20 Ma, in agreement with ages of 32–18 Ma obtained from strontium isotope stratigraphy within the underlying Asmari Formation (Ehrenberg *et al.*, 2007). According to James & Wynd (1965), the onset of siliclastic sedimentation in the Zagros basin started between 28 and 16 Ma. This is consistent with the age of the Razak Formation, which further marked the onset of the overfilled stage of the Zagros foreland. As such, we infer that the flexural development associated with the onset of the collision might have occurred before 20 Ma on the Arabian passive margin, as argued previously (Agard *et al.*, 2005; Mouthereau *et al.*, 2006; Ahmadhadi *et al.*, 2007). This event is consistent with the start of decreased plate convergence rates between Arabia and Eurasia near 25 Ma (McQuarrie *et al.*, 2003). We date the base of the Agha Jari Formation at 16.6 Ma, which is slightly older than the Agha Jari Formation at a similar structural position in the Izeh zone (NW of our studied area), where its base was dated magnetostratigraphically at ca. 15.5 Ma (Emami, 2008). This transition appears to be significantly older than at the mountain front in the Lorestan area, where it is dated at 12.8–12.3 Ma (Homke *et al.*, 2004).

Our magnestostratigraphic study indicates that the transition from Agha Jari to the lower Bakhtyari conglomerates (Bk1) is dated to 14.8 Ma (Fig. 8). This result contrasts with the long-lived tendency to assume a Pliocene age for the Bakhtyari conglomerates, but is consistent with a slightly older Miocene age recently proposed for a marine interval of the Bakhtyari conglomeratic succession based on the palaeontological and palynological content (Fakhari *et al.*, 2008). By extrapolating the sedimentation rate from the uppermost polarity reversal upwards in the section, the age of the top of the logged section can be roughly estimated to be 13.9 Ma (Fig. 8). At the scale of the foreland basin, part of these conglomerates might be the proximal equivalent to the Agha Jari Formation found in the southern coastal Fars. The overall southward migration of the sedimentation and the upward coarsening outline the evolution towards an overfilled foreland basin (e.g. Covey, 1986; Sinclair, 1997). Finally, taking into account that the Bakhtyari 1 conglomerates studied were deposited approximately at sea level, we infer that the uplift of the northern Zagros to its present-day elevation of 2000 m was achieved after 13.9 Ma.

Constraints in the timing of folding in the northern Fars

Two stages of folding have been previously described, but not accurately dated, in the study area (Mouthereau *et al.*, 2007). The first stage of folding corresponds to the growth of the Sorkh anticline. It is recorded by the growth strata within the Bk1 conglomerates on the northern flank of the Qalat syncline (Figs 3 and 10). Despite the lack of direct stratigraphic constraints within the Bk1 succession, an age for this folding can be determined assuming a simple correlation between similar depositional sequences, ages and

structural position (Fig. 1) at the scale of the overall studied area (15 × 15 km). The oldest growth strata are located close to the base of the Bk1 conglomerates. As a result, and if our hypothesis is correct, one can estimate an age of 14–15 Ma for the initiation of the Sorkh anticline and more generally for the folding in the northern ZFB. This new stratigraphic age indicates that this early folding stage is 3–9 Ma older than initially thought (Mouthereau *et al.*, 2007).

The second stage of folding is associated with the growth of the Derak anticline and the development of adjacent Chahar–Makan and Qalat synclines (Fig. 1). During this second stage of folding, the uppermost Bk1 conglomerates were tilted and sealed by the regional-scale unconformity outlined by the horizontal Bk2 alluvial conglomerates, which are not dated as yet (Figs 3 and 10). Unfortunately, growth strata related to this episode, if any, have not been preserved in the conglomeratic succession. Together with the drastic shift towards more continental conditions, this observation supports rapid uplift in a subaerial environment and limited coeval sedimentation. Although Mouthereau *et al.* (2007) proposed an age of 2–3 Ma for this stage, folding could have started at any time after 14–15 Ma. This calls for the need to gain more complete dating throughout the syn-orogenic deposits of the Zagros foreland basin. With regard to the kinematics of the studied structural units, it is worth noting that neither the ChRM (after tectonic correction) nor the postfolding remagnetization (before tectonic correction) shows a statistically significant deviation from the expected reference direction in the area (Fig. 7). This demonstrates the absence of significant vertical-axis rotations in the area studieddespite its location near the active Sabz–Pushan strike–slip fault (Fig. 1b). This result needs to be integrated with previously published (Aubourg *et al.*, 2008) palaeomagnetic results in the region in order to determine the pattern of regional-scale vertical-axis rotations in the western part of the Fars arc.

Early–Middle Miocene sedimentation rates and unroofing of the internal Zagros

The sedimentation rates derived from magnetostratigraphy show three main trends that follow the deposition of the Razak, Agha Jari and Bakhtyari formations (Fig. 8). The Razak Formation is characterized by mean sedimentation rates of 0.18 mm yr^{-1}. Sediments of this formation (bioclastic sediments, dolostones and blue mudstones) are indicative of marine sabkha environments, although interbedded red clays reveal some sporadic subaerial exposure. The Agha Jari Formation is characterized by slightly increasing mean sedimentation rates of 0.23 mm yr^{-1}. Larger clast sizes (up to 10 cm), and a significant fraction of chert and limestone pebbles originating from Mesozoic limestones, Eocene or Miocene limestones, indicate a source located in the High Zagros or close to the MZT. There, the radiolarian red cherts of the Mesozoic ophiolitic units have been eroded, transported and redeposited into the foreland basin from the Eocene until the Miocene (Fakhari *et al.*, 2008). This evidence indicates unroofing of the Neyriz ophiolites located in the northeast or much farther ophiolitic units found northwestwards in the Kermanshah area (Fig. 1a). This is consistent with the palaeocurrent orientations revealing south- to southeast-directed flows (Fig. 4). Finally, sedimentation rates increase significantly for the Bakhtyari 1 conglomerates, reaching a mean rate of 0.52 mm yr^{-1}. The abundance and the size of limestone clasts increase upwards to reach 30 cm at most. This indicates a more local source of sedimentation and implies the unroofing of more proximal units of the High Zagros where limestones are present. The occurrence of nummulitic pebbles in the Agha Jari and Bakhtyari 1 Formations argues for the erosion of the Jahrom Formation or the Asmari Formation currently exposed in the Sorkh anticline (Fig. 1b). This is consistent with the intraformational unconformity found within the Bk1 conglomerates and the dominant south-directed flows. The small-scale fan deltas transporting sediments from the Sorkh anticline likely fed the surrounding marine deltas situated at the current position of the Qalat and Chahar–Makan synclines. We thus infer that the Sorkh anticline located in the footwall of the High Zagros Fault may have emerged above sea level by about 14–15 Ma.

CONCLUSIONS

Magnetostratigraphy data presented here for the northern flank of the Chahar–Makan syncline provide new time constraints on the onset of foreland sedimentation and the initiation of folding in the northern part of the ZFB. The correlation of magnetic polarity sequences to the GPTS indicates that the deposition of synorogenic siliciclastic succession started as early as the Early Miocene at least 19.7 Ma ago, and corresponds to the Razak Formation in the Chahar–Makan syncline. The overlying Agha Jari Formation was deposited between 16.6 and 14.8 Ma. The deposition of the Bakhtyari 1 conglomerates started after 14.8 Ma. The sediment accumulation rates increase from 0.18 mm yr^{-1} in the Razak Formation to 0.52 mm yr^{-1} in the Bakhtyari Formation (Bk1) at the top of the studied section.

The onset of deformation in the northern Zagros likely started around 14–15 Ma and was associated with growth strata at the base of the Bk1 succession found in the northern limb of the Qalat syncline. We suggest that the onset of folding might be related to the rapid (nearly instantaneous) propagation associated with the buckling of the sedimentary cover as previously proposed (Lacombe *et al.*, 2007; Mouthereau *et al.*, 2007). A second stage of folding reveals increasing contraction marked by the change towards more continental environmental conditions. This phase is found in association with the growth of the Derak anticline and produced tilting of the Bk1 conglomerates. The Bk1 conglomerates are truncated by an erosional surface on top of which Bk2 conglomerates are deposited uncon-

formably. Although new dating campaigns are necessary to unravel the age of the Bk1/Bk2 unconformity, this study reveals that tectonic deformation was already ongoing in the Middle–Upper Miocene in the northern part of the ZFB.

ACKNOWLEDGEMENTS

This work greatly benefited from the support of the Geological Survey of Iran (Tehran and Shiraz) during the extensive field work in Iran. The authors would like to especially thank M.A. Sedaghat, manager of Shiraz headquarter. We are grateful to Miguel Garcés, who provided insightful comments during the analysis of the palaeomagnetic results. The authors greatly acknowledge the ISIS program, which provided SPOT 5 × 5 m resolution images. This work was funded by CNRS, UPMC and the Franco-Spanish Picasso PHC programme. We also thank Mark Allen and two anonymous reviewers, as well as Editor Peter van der Beek for their helpful comments that helped to improve the manuscript.

REFERENCES

Agard, P., Omrani, J., Jolivet, L. & Mouthereau, F. (2005) Convergence history across Zagros (Iran): constraints from collisional and earlier deformation. *Int. J. Earth Sci.*, **94**, 401–419.

Ahmadhadi, F., Lacombe, O. & Daniel, J.-M. (2007) Early Reactivation of Basement Faults in Central Zagros (Sw Iran): Evidence from Pre-Folding Fracture Populations in Asmari Formation and Lower Tertiary Paleogeography. In: *Thrust Belts and Foreland Basins: From Fold Kinematics to Hydrocarbon Systems* (Ed. by O. Lacombe, J. Lavé, J. Verges & F. Roure) *Front. Earth Sci.*, 205–228. Springer-Verlag, Berlin.

Allen, M.B. & Armstrong, H.A. (2008) Arabia-Eurasia collision and the forcing of mid-Cenozoic global cooling. *Palaeogeogr. Palaeoclimatol. Palaeoecol.*, **265**, 52–58.

Ambraseys, N.N. & Melville, C.P. (1982) *A History of Persian Earthquakes*. Cambridge University Press, Cambridge, UK.

Aubourg, C., Smith, B., Bakhtari, H.R., Guya, N. & Eshraghi, A. (2008) Tertiary block rotations in the Fars Arc (Zagros, Iran). *Geophys. J. Int.*, **173**, 659–673.

Berberian, F. & Berberian, M. (1981) Tectono-Plutonic episodes in Iran. In: *Zagros-Hindu Kush-Himalaya Geodynamic Evolution* (Ed. by H.K. Gupta & F.M. Delany) *Geodyn. Ser.*, **3**, 5–32. American Geophysical Union, Washington, DC.

Berberian, F., Muir, I.D., Pankhurst, R.J. & Berberian, M. (1982) Late cretaceous and early Miocene Andean-type plutonic activity in Northern Makran and Central Iran. *J. Geol. Soc. Lond.*, **139**, 605–614.

Berberian, M. (1995) Master "Blind" Thrust Faults Hidden under the Zagros Folds: active basement tectonics and surface tectonics surface morphotectonics. *Tectonophysics*, **241**, 193–224.

Berberian, M. & King, G.C.P. (1981) Towards a paleogeography and tectonic evolution of Iran. *Can. J. Earth Sci. = J. Can. Sci. Terre*, **18**, 210–265.

Beydoun, Z.R., Clarke, M.W.H. & Stoneley, R. (1992) Petroleum in the Zagros Basin; a Late Tertiary Foreland Basin overprinted onto the outer edge of a vast hydrocarbon-rich paleozoic-mesozoic passive-margin shelf. In: *Foreland Basins and Fold Belts* (Ed. by R.W. Macqueen & D.A. Leckie), *AAPG Mem.* **55**, 309–339.

Burbank, D.W., Puigdefàbregas, C. & Muñoz, J.A. (1992) The chronology of eocene tectonic and stratigraphic development of the Eastern Pyrenean Foreland Basin, Northeast Spain. *Geol. Soc. Am. Bull.*, **104**, 1101–1120.

Burbank, D.W. & Reynolds, R.G.H. (1988) Stratigraphic keys to the timing of thrusting in Terrestrial Foreland Basins: applications of the Northwestern Himilaya. In: *New Perspectives in Basin Analysis* (Ed. by K.L. Kleinspehn & C. Paola), pp. 331–351. Springer-Verlag, New York.

Colman-Sadd, S. (1978) Fold development in Zagros Simply Folded Belt, Southwest Iran. *Am. Assoc. Petrol. Geol. Bull.*, **62**, 984–1003.

Covey, M. (1986) The evolution of Foreland Basins to Steady State: evidence from the Western Taiwan Foreland Basin. *Spec. Publ. Int. Assoc. Sedimentol.*, **8**, 77–90.

Ehrenberg, S.N., Pickard, N.A.H., Laursen, G.V., Monibi, S., Mossadegh, Z.K., Svånå, T.A., Aqrawi, A.A.M., McArthur, J.M. & Thirlwall, M.F. (2007) Strontium isotope stratigraphy of the Asmari Formation (Oligocene-Lower Miocene), Sw Iran. *J. Petrol. Geol.*, **30**, 107–128.

Emami, H. (2008) *Foreland Propagation of Folding and Structure of the Mountain Front Flexure in the Pusht-E Kuh Arc (Zagros, Iran)*. Universitat de Barcelona, Barcelona.

Fakhari, M.D., Axen, G.J., Horton, B.K., Hassanzadeh, J. & Amini, A. (2008) Revised age of proximal deposits in the Zagros Foreland Basin and implications for Cenozoic evolution of the High Zagros. *Tectonophysics*, **451**, 170–185.

Heermance, R.V., Chen, J., Burbank, D.W. & Wang, C. (2007) Chronology and tectonic controls of Late Tertiary Deposition in the Southwestern Tian Shan Foreland, Nw China. *Basin Res.*, **19**, doi:10.1111/j.1365-2117.2007.00339.x.

Hempton, M.R. (1987) Constraints on Arabian Plate motion and extensional history of the Red Sea. *Tectonics*, **6**, 687–705.

Homke, S., Vergés, J., Garcés, M., Emami, H. & Karpuz, R. (2004) Magnetostratigraphy of Miocene–Pliocene Zagros Foreland deposits in the front of the Push-E Kush Arc (Lurestan Province, Iran). *Earth Planet. Sci. Lett.*, **225**, 397–410.

Homke, S., Vergés, J., Serra-Kiel, J., Bernaola, G., Garcés, M., Montero-Verdú, I.M., Sharp, I., Karpuz, R. & Goodarzi, M.H. (2009) Formation of the early Zagros Foreland Basin: biostratigraphic and Magnetostratigraphic evidence from the Paleocene Amiran, Taleh Zang and Kashkan Formations of Lurestan Province, Sw Iran. *Geol. Soc. Am. Bull.*, **121**, 963–978.

Homke, S., Vergès, J., Van der Beek, P.A., Fernandez, M., Saura, E., Barbero, L., Badics, B. & Labrin, E. Insights in the exhumation history of the Nw Zagros from Bedrock and Detrital Apatite Fission-Track Analysis: evidence for a long-lived orogeny. *Basin Res.*, doi: 10.1111/j.1365-2117.2009.00431.x.

Horton, B.K., Hassanzadeh, J., Stockli, D.F., Axen, G.J., Gillis, R.J., Guest, B., Amini, A., Fakhari, M., Zamanzadeh, S.M. & Grove, M. (2008) Detrital Zircon Provenance of Neoproterozoic to Cenozoic Deposits in Iran: implications for Chronostratigraphy and Collisional Tectonics. *Tectonophysics*, **451**, 97–122.

James, G.A. & Wynd, J.G. (1965) Stratigraphic nomenclature of Iranian oil consortium agreement area. *Am. Assoc. Petrol. Geol. Bull.*, **49**, 2162–2245.

Jordan, T.E. & Alonso, R.N. (1987) Cenozoic stratigraphy and Basin Tectonics of the Andes Mountains, 20–28° South Latitude. *Am. Assoc. Petrol. Geol. Bull.*, **71**, 49–64.

Kirschvink, J.L. (1980) The least-squares line and plane and the analysis of Paleomagnetic data. *Geophys. J. R. Astronom. Soc.*, **62**, 699–718.

Koop, W. & Stoneley, R. (1982) Subsidence history of the Middle East Zagros Basin, Permian to recent. *Phil. Trans. R. Soc. Lond.*, **305**, 149–168.

Lacombe, O., Amrouch, K., Mouthereau, F. & Dissez, L. (2007) Calcite twinning constraints on Late Neogene stress patterns and deformation mechanisms in the Active Zagros Collision Belt. *Geology*, **35**, 263–266.

Larrasoaña, J.C., Murelaga, X. & Garcés, M. (2006) Magnetobiochronology of Lower Miocene (Ramblian) Continental Sediments from the Tudela Formation (Western Ebro Basin, Spain). *Earth Planet. Sci. Lett.*, **243**, 409–423.

Lourens, L.J., Hilgen, F.J., Shackleton, N.J., Laskar, J. & Wilson, D. (2004) The Neogene period. In: *A Geological Time Scale 2004* (Ed. by F.M. Gradstein, J.G. Ogg & A.G. Smith), pp. 409–440. Cambridge University Press, Cambridge, UK.

McFadden, P.L. & McElhinny, M.W. (1990) Classification of the reversal test in palaeomagnetism. *Geophys. J. Int.*, **103**, 725–729.

McQuarrie, N. (2004) Crustal Scale geometry of the Zagros Fold-Thrust Belt, Iran. *J. Struct. Geol.*, **26**, 519–535.

McQuarrie, N., Stock, J.M., Verdel, C. & Wernicke, B.P. (2003) Cenozoic evolution of neotethys and implications for the causes of plate motions. *Geophys. Res. Lett.*, **30**, doi: 10.1029/2003GL017992.

Molinaro, M., Guezou, J.C., Leturmy, P., Eshraghi, S.A. & Frizon de Lamotte, D. (2004) The origin of changes in structural style across the Bandar Abbas Syntaxis, Se Zagros (Iran). *Mar. Petrol. Geol.*, **21**, 735–752.

Molinaro, M., Leturmy, P., Guezou, J.-C., Frizon de Lamotte, D. & Eshraghi, S.A. (2005) The structure and kinematics of the South-Eastern Zagros Fold-Thrust Belt; Iran: from thin-skinned to thick-skinned tectonics. *Tectonics*, **24**, doi: 10.1029/2004TC001633.

Motiei, H. (1993) *Geology of Iran: Stratigraphy of Zagros*. Geological Survey of Iran, Tehran.

Mouthereau, F., Lacombe, O. & Meyer, B. (2006) The Zagros Folded Belt (Fars, Iran): constraints from topography and critical wedge modelling. *Geophys. J. Int.*, **165**, 336–356.

Mouthereau, F., Tensi, J., Bellahsen, N., Lacombe, O. & Kargar, S. (2007) Tertiary sequence of deformation in a thin-skinned/thick-skinned collision belt: the Zagros Folded Belt (Fars, Iran). *Tectonics*, **26**, doi: 10.1029/2007TC002098.

Oveisi, B., Lavé, J., Van der Beek, P., Carcaillet, J., Benedetti, L. & Aubourg, C. (2009) Thick- and thin-skinned deformation rates in the Central Zagros Simple Folded Zone (Iran) indicated by displacement of geomorphic surfaces. *Geophys. J. Int.*, **176**, 627–654.

Raffi, I., Backman, J., Fornaciari, E., Pälike, H., Rio, D., Lourens, L. & Hilgen, F. (2006) A review of calcareous nannofossil astrobiochronology encompassing the past 25 million years. *Quat. Sci. Rev.*, **25**, 3113–3137.

Reynolds, J.H., Jordan, T.E., Johnson, N.M., Damanti, J.F. & Tabbutt, K.D. (1990) Neogene deformation of the Flat-Subduction Segment of the Argentine–Chilean Andes: magnetostratigraphic constraints from Las Juntas, La Rioja Province, Argentina. *Geol. Soc. Am. Bull.*, **102**, 1607–1622.

Schlunegger, F., Matter, A., Burbank, D.W. & Klaper, E.M. (1997) Magnetostratigraphic constraints on relationships between evolution of the Central Swiss Molasse Basin and Alpine Orogenic events. *Geol. Soc. Am. Bull.*, **109**, 225–241.

Sherkati, S. & Letouzey, J. (2004) Variation of structural style and Basin Evolution in the Central Zagros (Izeh Zone and Dezful Embayment), Iran. *Mar. Petrol. Geol.*, **21**, 535–554.

Sinclair, H.D. (1997) Tectonostratigraphic model for underfilled peripheral Basins: an Alpine perspective. *Geol. Soc. Am. Bull.*, **109**, 324–346.

Smith, B., Aubourg, C., Guezou, J.C., Nazari, H., Molinaro, M., Braud, X. & Guya, N. (2005) Kinematics of a Sigmoidal fold and vertical axis rotation in the East of the Zagros–Makran Syntaxis (Southern Iran): paleomagnetic, magnetic fabric and microtectonic approaches. *Tectonophysics*, **411**, 89–109.

Stocklin, J. (1968) Structural history and tectonics of Iran; a review. *Am. Assoc. Petrol. Geol. Bull.*, **52**, 1229–1258.

Stoneley, R. (1981) The geology of the Kuh-E Dalneshin Area of Southern Iran, and Its bearing on the evolution of Southern Tethys. *J. Geol. Soc. Lond.*, **138**, 509–526.

Stoneley, R. (1990) The Arabian Continental Margin in Iran During the Late Cretaceous. In: *The Geology and Tectonics of the Oman Region* (Ed. by A.H.F. Robertson, M.P. Searle & A.C. Ries), pp. 787–795. Geological Society of London, London.

Vernant, P., Nilforoushan, F., Hatzfeld, D., Abbassi, M.R., Vigny, C., Masson, F., Nankali, H., Martinod, J., Ashtiani, A., Bayer, R., Tavakoli, F. & Chéry, J. (2004) Present-Day crustal deformation and plate kinematics in the Middle East constrained by Gps measurements in Iran and Northern Oman. *Geophys. J. Int.*, **157**, 381–398.

Vincent, S.J., Allen, M.B., Ismail-Zadeh, A.D., Flecker, R., Foland, K.A. & Simmons, M.D. (2005) Insights from the Talysh of Azerbaijan into the paleogene evolution of the South Caspian Region. *Geol. Soc. Am. Bull.*, **117**, 1513–1533.

Ziegler, M.A. (2001) Late Permian to holocene paleofacies evolution of the Arabian Plate and Its hydrocarbon occurrences. *GeoArabia*, **6**, 445–503.

Zijderveld, J.D.A. (1967) A.C. demagnetization of rocks: analysis of results. In: *Methods in Paleomagnetism* (Ed. by D.W. Collinson, K.M. Creer & S.K. Runcorn), pp. 254–286. Elsevier, Amsterdam.

Manuscript received 26 April 2009; Manuscript accepted 2 October 2009.